NASA CR 137547
ASRL TR 174-3

WIND TUNNEL GENERATION OF SINUSOIDAL LATERAL AND LONGITUDINAL GUSTS BY CIRCULATION CONTROL OF TWIN PARALLEL AIRFOILS

Norman D. Ham
Paul H. Bauer
Thomas L. Lawrence

August 1974

Prepared under Contract No. NAS2-7262 by

Aeroelastic and Structures Research Laboratory
Department of Aeronautics and Astronautics
Massachusetts Institute of Technology
Cambridge, Massachusetts 02139

for

AMES RESEARCH CENTER
NATIONAL AERONAUTICS AND SPACE ADMINISTRATION
MOFFETT FIELD, CALIFORNIA 94035

NASA CR 137547
ASRL TR 174-3

WIND TUNNEL GENERATION OF SINUSOIDAL LATERAL AND LONGITUDINAL GUSTS BY CIRCULATION CONTROL OF TWIN PARALLEL AIRFOILS

Norman D. Ham
Paul H. Bauer
Thomas L. Lawrence

August 1974

Prepared under Contract No. NAS2-7262 by

Aeroelastic and Structures Research Laboratory
Department of Aeronautics and Astronautics
Massachusetts Institute of Technology
Cambridge, Massachusetts 02139

for

AMES RESEARCH CENTER
NATIONAL AERONAUTICS AND SPACE ADMINISTRATION
MOFFETT FIELD, CALIFORNIA 94035

1. Report No.	2. Government Accession No.	3. Recipient's Catalog No.
NASA CR-137547		

4. Title and Subtitle	5. Report Date
WIND TUNNEL GENERATION OF SINUSOIDAL LATERAL AND LONGITUDINAL GUSTS BY CIRCULATION CONTROL OF TWIN PARALLEL AIRFOILS	August 1974
	6. Performing Organization Code

7. Author(s)	8. Performing Organization Report No.
Norman D. Ham Paul H. Bauer Thomas L. Lawrence	ASRL TR 174-3
	10. Work Unit No.

9. Performing Organization Name and Address	11. Contract or Grant No.
Massachusetts Institute of Technology Aeroelastic and Structures Research Laboratory Cambridge, Massachusetts 02139	NAS2-7262
	13. Type of Report and Period Covered
12. Sponsoring Agency Name and Address	Contractor Report
National Aeronautics and Space Administration Moffett Field, California 94035	14. Sponsoring Agency Code

15. Supplementary Notes

NASA Technical Monitors: J.P. Rabbott, Jr., and Wayne R. Johnson

16. Abstract

A gust generator capable of producing sinusoidal lateral and longitudinal gusts has been developed for the purpose of studying the gust response of a model rotor-propeller in the MIT Wright Brothers Wind Tunnel.

This gust generator utilizes harmonic circulation control of twin parallel airfoils to achieve the harmonic lift variation required for gust generation.

The gust generator design, construction, and testing is described. Typical test results are presented in the form of lateral and longitudinal gust perturbation velocities as a function of generator reduced frequency.

17. Key Words (Suggested by Author(s))	18. Distribution Statement
Circulation Control Gust Generators Wind Tunnels	Unclassified, Unlimited

19. Security Classif. (of this report)	20. Security Classif. (of this page)	21. No. of Pages	22. Price*
Unclassified	Unclassified	37	

* For sale by the National Technical Information Service, Springfield, Virginia 22151

FOREWORD

This report has been prepared by the Aeroelastic and Structures Research Laboratory (ASRL), Department of Aeronautics and Astronautics, Massachusetts Institute of Technology, Cambridge, Massachusetts, under NASA Contract No. NAS2-7262 from the Ames Research Center, National Aeronautics and Space Administration, Moffett Field, California 94035. Mr. John Rabbott and Dr. Wayne Johnson of the Ames Research Center served as technical monitors. The valuable assistance and advice received from these individuals is gratefully acknowledged.

ABSTRACT

A gust generator capable of producing sinusoidal lateral and longitudinal gusts has been developed for the purpose of studying the gust response of a model rotor-propeller in the MIT Wright Brothers Wind Tunnel.

This gust generator utilizes harmonic circulation control of twin parallel airfoils to achieve the harmonic lift variation required for gust generation.

The gust generator design, construction, and testing is described. Typical test results are presented in the form of lateral and longitudinal gust perturbation velocities as a function of generator reduced frequency.

CONTENTS

SECTION 1

INTRODUCTION

The simulation of sinusoidal lateral and longitudinal gusts in the wind tunnel is difficult to achieve with a simple device over the range of frequencies and amplitudes of interest.

A number of investigators have developed methods of generating sinusoidal lateral gusts using various arrangements of oscillating vanes or airfoils with oscillating jet flaps in slotted, open, and closed test sections.[1-5] In some cases the technique used is applicable to the generation of sinusoidal longitudinal gusts. The techniques of References 3 and 4 are of particular interest, since they utilize oscillating jet flaps having a minimum of vibrating mechanism and therefore a high frequency capability, do not require major modifications to the test section, and are capable of generating both lateral and longitudinal gusts. However, they both require quite large jet momentum coefficients to achieve acceptable gust amplitudes.

Since the available air supply in the Wright Brothers Wind Tunnel at MIT is of modest capacity, it was decided to apply the principle of airfoil circulation control to obtain the oscillating lift necessary for gust generation. By this means it was possible to reduce the required jet momentum coefficients by an order of magnitude.

The method of approach was taken from the work described in Reference 6, which utilized a hollow elliptical airfoil having two blowing slots at the rear, formed by truncating the elliptic section, and fitting a circular cylinder into the resulting gap. The interior of the airfoil was divided into two plenum chambers, one supplying each slot. Tests were conducted with blowing from one or both slots. Large lift coefficients were generated at relatively small jet momentum coefficients C_μ, where

$$C_\mu = \frac{T}{qc}$$

and

T = slot thrust

q = free-stream dynamic pressure

c = airfoil chord

In the present application, oscillating lift was obtained by eccentrically mounting the trailing edge cylinder and rotating it in such a manner that the slots alternately opened and closed, as described in detail in Section 3.

The considerations that led to the final design configuration are described in the following section.

SECTION 2

DESIGN CONSIDERATIONS

The following model is suggested in the literature for the power spectral density of longitudinal velocity fluctuations resulting from isotropic atmospheric turbulence[7]:

$$\phi_u(\omega_r) = \sigma_u^2 \frac{2L}{\pi} \frac{1}{[1 + (1.34\omega_r L)^2]^{5/6}}$$

where σ_u = standard deviation of longitudinal turbulence velocity

L = turbulence scale length

ω_r = spacewise circular frequency

A similar model is suggested for lateral velocity fluctuations.

The complete simulation of these models of atmospheric turbulence in the wind tunnel is obviously impossible. However, a reasonable representation at selected frequencies is possible using the technique described below.

Consider the arrangement shown in Figure 2. Twin vertical airfoils at zero incidence are mounted symmetrically to the left and right of the wind-tunnel centerline. The trailing edge portion of each airfoil consists of an oscillatory circulation control assembly driven by an electric motor (see Section 3). Any desired frequency of airfoil sinusoidal lift variation can be prescribed by control of motor rotational speed.

Assume in this instance that the sinusoidal lift variation of the two airfoils occurs at frequency ω and out-of-phase by 180 degrees. Then each airfoil will shed a time-varying vortex wake which will induce incremental longitudinal and vertical velocities over the region between the airfoils $u(x,h,t)$ and $w(x,h,t)$, respectively. If the lift variation is 180 degrees out-of-phase,

it is seen from Figure 1 that the velocities w(x,h,t) due to the wakes of both flaps cancel exactly at the tunnel centerline and nearly cancel elsewhere, while the velocities u(x,h,t) are additive. The presence of the tunnel walls can be accounted for in the theoretical analysis by the method of images.*

It can be shown that the distribution of perturbation velocities generated far downstream in a rectangular wind tunnel is given by

$$\frac{u}{VC_\ell} = k \frac{\sinh k\bar{h}_1}{\sinh k\bar{h}_w} \cosh k\bar{\ell} \sin\omega t$$

$$\frac{v}{VC_\ell} = k \frac{\sinh k\bar{h}_1}{\sinh k\bar{h}_w} \sinh k\bar{\ell} \sin\omega t$$

in the out-of-phase case, and

$$\frac{u}{VC_\ell} = k \frac{\sinh k\bar{h}_1}{\cosh k\bar{h}_w} \sinh k\bar{\ell} \sin\omega t$$

$$\frac{v}{VC_\ell} = k \frac{\sinh k\bar{h}_1}{\cosh k\bar{h}_w} \cosh k\bar{\ell} \sin\omega t$$

in the in-phase case, where

u = perturbation longitudinal velocity amplitude
v = perturbation lateral velocity amplitude
V = tunnel velocity
C_ℓ = airfoil lift-coefficient amplitude
k = reduced frequency of lift variation $\omega b/V$
ω = frequency of lift variation
b = airfoil semichord

*This portion of the analysis is due to W.Johnson, Ames Research Center.

$\bar{h}_1$ = non-dimensional distance from wall to airfoil, h_1/b

$\bar{h}_w$ = non-dimensional distance from wall to tunnel centerline, h_w/b

$\bar{\ell}$ = non-dimensional distance from tunnel centerline, ℓ/b

The gust generator design was governed by the following considerations:

1. The test section of the Wright Brothers Wind Tunnel has an oval cross-section ten feet wide and seven feet high.
2. The model to be tested was a rotor-propeller, having a diameter of three feet, in the cruise mode.
3. The available tunnel air supply was limited in flow rate.
4. The design advance ratio of the rotor-propeller was to be unity.
5. The gust frequency range of interest was from zero to 1.5/revolution in terms of rotor rotational speed.
6. Airfoil spacing was to be two rotor diameters to avoid interference of the airfoil wakes with the rotor.
7. The maximum gust incremental velocities were to be five percent of free stream at a tunnel speed of 120 feet per second.

At an advance ratio of unity, i.e.,

$$\frac{V}{\Omega R} = 1 \ ,$$

rotor rotational speed is given by

$$\Omega = \frac{V}{R}$$

At a frequency ratio of 1.5, i.e.,

$$\frac{\omega}{\Omega} = 1.5,$$

the gust frequency is

$$\omega = 1.5\Omega = 1.5\frac{V}{R}$$

Then the upper limit on gust generator reduced frequency is

$$k_{max} = \frac{\omega b}{V} = 1.5\ \frac{V}{R}\frac{b}{V} = 1.5\ \frac{b}{R}$$

It is desirable to keep the reduced frequency low to minimize flow distortion over the rotor disk. On the other hand, the incremental gust velocities are proportional to kC_ℓ, and since from Reference 6

$$C_\ell \sim C_\mu^{1/2}$$

then

$$kC_\ell \sim (\text{chord})^{1/2}$$

Since the tunnel air supply was limited, the airfoil chord was sized by the requirement to achieve maximum gust incremental velocities of five percent of free stream at the design tunnel speed of 173 feet per second.

The above considerations led to the following gust generator parameters:

$$b = 1 \text{ ft}$$
$$h_1 = 2 \text{ ft}$$
$$h_w = 5 \text{ ft}$$

The detail design of the gust generator is described in the following section.

SECTION 3

MECHANICAL DESCRIPTION AND TEST PROCEDURE

3.1 Introduction

The gust generator described in this study uses two identical airfoils. A method for producing high-frequency, sinusoidal variations of the lift of each airfoil is required. The high frequencies precluded oscillating the airfoils or even a blown flap mounted on the airfoils. The available air supply also placed restrictions on the possible alternatives. It was determined that the requirements could be met by a special form of circulation-controlled airfoil (CCA).

A typical CCA has a thick section (15-50% chord), moderate camber , and a blunt trailing edge having an upper slot (see Figure 2a). Pressurized air ejected from the slot delays upper surface boundary-layer separation, moving the stagnation point to the underside of the trailing edge and creating lift. The amount of lift generated is governed by the jet-momentum coefficient, C_μ. Such an airfoil can produce lift at zero angle of attack, and is also capable of generating a lift coefficient near the theoretical maximum.

R.J. Kind has experimented with a somewhat different form of CCA.[6] (See Figure 2b). It has an elliptical section, zero camber, and both an upper and a lower blowing slot. The position of the stagnation point is then governed by ΔC_μ, the difference between the upper and the lower C_μ's. For the present application, the primary advantage of such a symmetrical CCA is that it produces positive or negative lift equally well. A method of rapidly varying ΔC_μ would then produce a lift variation suitable for present purposes. Such a method, using a rotating cylinder to act as an air valve, is described below.

3.2 General Description

The basic design of the CCA used is shown in Figure 3. It is an elliptical section airfoil, modified by the addition of a rotatable cylinder recessed into the trailing edge. The cylinder is smaller in diameter than the width of the channel containing it, and the resulting gaps form the upper and the lower blowing slots. Most importantly, the cylinder is eccentrically mounted to act as a cam. The channel width, cylinder diameter and eccentricity are chosen so that the "lobe" of the cylinder completely closes each slot once per revolution. The channel also forms a secondary plenum forward of the cylinder, and it, in turn, is connected by air passages to the primary plenum inside of the airfoil.

Figure 4 shows the operation of the cylinder. Low pressure air is fed to the wing and pressurizes the primary and secondary plenums. In Figure 4a, the cylinder lobe is at zero degrees, the upper and lower slots have the same size, ($t_u = t_\ell$), $\Delta C_\mu = 0$, and no lift is generated. Figure 4b shows the cylinder lobe at 45 degrees, $t_\ell > t_u$, ΔC_μ is negative and the wing is producing negative (downward) lift. By the time the lobe gets to 90 degrees, Figure 4c, t_ℓ is maximum, $t_u = 0$, ΔC_μ is maximum negative and maximum negative lift is produced. The cylinder continues to rotate, opening the upper slot, closing the lower, until at 180 degrees, Figure 4d, $t_u = t_\ell$ and the wing have returned to zero lift. As the cylinder completes its revolution, the lower gap is now decreased, the upper gap increased, and at 270 degrees Figure 4e, maximum positive lift is produced. Finally, in Figure 4f, the cylinder is at 360 degrees, and the cycle begins again.

The airfoil configuration chosen has several advantages:

1) The ability to operate at high frequency
2) Mechanical simplicity since the only moving part is the rotating cylinder

3) The capability of generating a high lift coefficient at low jet momentum coefficients.

3.3 Detailed Description

The two CCA that comprise the gust generator are identical, elliptical section, constant chord wings of 66-inch span and 25.9-inch chord. The section has zero camber, 20% thickness/chord ratio, and 7.7% cylinder diameter/chord ratio. The cylinder center is mounted at the 96% chord position. The thickness ratio, cylinder size, and cylinder position were chosen to match that of Reference 6, while the span was dictated by the size of the test section of the Wright Brothers Wind Tunnel (7 by 10-foot oval).

The primary structure of the wing consists of a forward spar at 50% chord, an aft channel (spar) at 90% chord and two tip ribs. (See Figure 5). The portion ahead of the spar consists of simple mahogany fairing, while the space between the spar and the channel forms the primary plenum.

The slot width was determined by an initial measurement that showed the air supply capable of providing a flow velocity of 700 feet per second through a two-square-inch opening. Since that was the desired slot velocity, the total gap (upper plus lower) was set at a convenient 0.020 inches, for a total slot area (both airfoils) of 2.5-square inches.

The cylinder itself is made from thick wall 4130 steel tubing, centerless ground to an outside diameter of 1.980 inches. It is divided into four equal spanwise segments, supported by three intermediate and two tip bearings. In order to provide for eccentric mounting, the ends of the cylinder segments were bored out and fitted with aluminum bushings having 7/8-inch holes offset 0.010 inch from the center.

The trailing-edge channel was divided into four equal segments, with intermediate bearing supports between the segments.

The channels were machined from aluminum. The cavity width is 2.000 inches, and in conjunction with the cylinder outside diameter of 1.980 inches and eccentricity of 0.010 inch, provides for the desired slot width and closure. The cavity is deeper than necessary and acts as a secondary plenum. Half-inch holes on three-quarter-inch spacing are drilled through the channel to connect primary and secondary plenums.

The channels and intermediate bearing supports are tied together by bolted-in splicing plates. These allow the channels to be centered over the cylinder during assembly so that equal upper and lower slot widths can be adjusted. The adjustment guarantees that alignment will be maintained after assembly of the wing is completed.

To keep the trailing edge as aerodynamically clean as possible, the intermediate bearing supports carry small diameter roller bearings recessed into the ends of the cylinders. Figure 6 shows a cross section through a typical bearing support. The support is made from half-inch carbon steel stock. The roller bearing rides on a 7/8-inch steel shaft that acts as an inner race. The shaft is fitted into the eccentric aluminum bushings of the adjacent cylinders. The cylinder, bushing, and shaft are pinned together to ensure that all bushings are eccentric in the same direction and that all four cylinder segments are synchronized. In addition, holes are drilled into the aluminum bushings to carry balancing weights. An O-ring on the cylinder face runs against a teflon washer inset in the bearing support to maintain a pressure seal.

The forward spar is a simple rectangular section aluminum bar. Holes are drilled through for the attachment of the mahogany fairing, while the ends are inset into the tip ribs by 3/8 inch for added rigidity.

The tip ribs are cut out of one-inch aluminum plate. Two

2-1/2-inch air inlets are cut in the aft portion. The trailing edge of the rib carries a ball bearing mounted in a holder adjustable for preload. On one end of the wing, the ball bearing rides on a stub shaft coming out of the end cylinder, while on the other, an extended shaft is used to connect the cylinder to the drive mechanism.

The wing skin over the aft portion must hold the primary plenum pressure. It is, therefore, made from 1/4-inch aluminum plate, bent to the elliptical contour. Because of the skin thickness, no internal ribs are used, but equally-spaced tie-bolts hold the skins together at 70% chord.

3.4 Mounting and Test Procedure

Figures 7 and 8 show the gust generator airfoils mounted in the Wright Brothers Wind Tunnel. They are mounted vertically and have a separation of six feet. Air is supplied to a large manifold of six-inch PVC pipe and then to the upper and lower tip ribs of each wing by four-inch PVC pipe runners. A D.C. motor, mounted on top of the tunnel, drives the cylinders by means of timing belts and pulleys.

Perturbation velocity measurements were made by an "x" configuration hot-wire anemometer probe. The wind tunnel is run at a series of speeds. At each speed, the flow velocity and perturbation are measured for a series of cylinder rotational speeds. This is done for the cylinders synchronized in-phase to produce lateral gusts, and then for the cylinders 180 degrees out-of-phase to produce longitudinal gusts.

SECTION 4

DISCUSSION OF RESULTS

Since testing was conducted at constant air supply mass flow and pressure, the jet momentum coefficient C_μ of the airfoils varied inversely as the square of tunnel velocity. Then from the results of Reference 6, the airfoil lift coefficient, C_ℓ varies approximately with C_μ as

$$C_\ell \sim C_\mu^{1/2}$$

Therefore,

$$C_\ell \sim \frac{1}{V}$$

From the theory of Section 2 for this case

$$\frac{u}{V} \text{ or } \frac{v}{V} \sim C_\ell \sim \frac{1}{V}$$

Therefore, the ratio of perturbation velocity to tunnel velocity should vary inversely with tunnel velocity for constant air flow and pressure.

The experimental results indicated such an inverse variation with tunnel velocity. Typical experimental results at tunnel center are shown in Figures 9 and 10 for tunnel speeds of 40, 60, 82.5, 100, and 120 miles per hour. The corresponding total plenum volume flow was 800 cubic feet per minute at a plenum pressure of 4 pounds per square inch. Shown for comparison in each figure is a theoretical curve for the case V = 82.5. Since the airfoil lift coefficient C_ℓ was unknown, the theoretical curve in each figure was arbitrarily matched to the experimental point at reduced frequency k of 0.6. It is seen that the theoretical curves predict the experimental trends fairly well.

The experimental distributions of longitudinal and lateral gust perturbation velocities over a four-foot square centered on

the tunnel center line are shown in Figures 11, 12, 13 and 14 for reduced frequencies of 0.5 and 1.0. The theoretical curves shown were arbitrarily matched to an experimental point on the line x = 0. The theoretical prediction of the lateral distributions is seen to be reasonable. The scatter in the data is presumably due to tunnel flow peculiarities.

The theory of Section 2 indicated that during the generation of longitudinal gusts, lateral gust components would occur at points not equidistant from the two generator airfoils, and vice versa. The experimental distributions of these cross-velocities is shown in Figures 15, 16, 17, and 18 for reduced frequencies of 0.5 and 1.0. The theoretical curves shown were arbitrarily matched to an experimental point on the line x = 0. For unknown reasons, the theory overpredicts the lateral distribution of the cross-velocities.

REFERENCES

1. Abbott, F.T., "Brief Description of the Characteristics of the Langley Transonic Dynamic Tunnel Airstream Oscillator", Paper 6, September 1968, NASA.

2. Buell, D.A., "An Experimental Investigation of the Velocity Fluctuations Behind Oscillating Vanes", NASA TN D-5543, November 1969.

3. Simmons, J.M., and Platzer, M.F., "Experimental Investigations of Incompressible Flow Past Airfoils with Oscillating Jet Flaps", Journal of Aircraft, 8, 8, August 1971.

4. Poisson-Quinton, P. "Note on a New V/STOL Rig in the S1 Modane Sonic Tunnel", ONERA presentation at the Third AGARD Meeting on V/STOL Tunnels, Amsterdam, February 1972.

5. Bicknell, J., and Parker, A.G., "A Wind-Tunnel Stream Oscillation Apparatus", Journal of Aircraft, 9, 6, June 1972.

6. Kind, R.J., and Maull, D.J., "An Experimental Investigation of a Low-Speed Circulation-Controlled Aerofoil", The Aeronautical Quarterly, May 1968.

7. Houbolt, J.C., Steiner, R., and Pratt, K.G., "Dynamic Response of Airplanes to Atmospheric Turbulence Including Flight Data on Input and Response", NASA R-199, 1964.

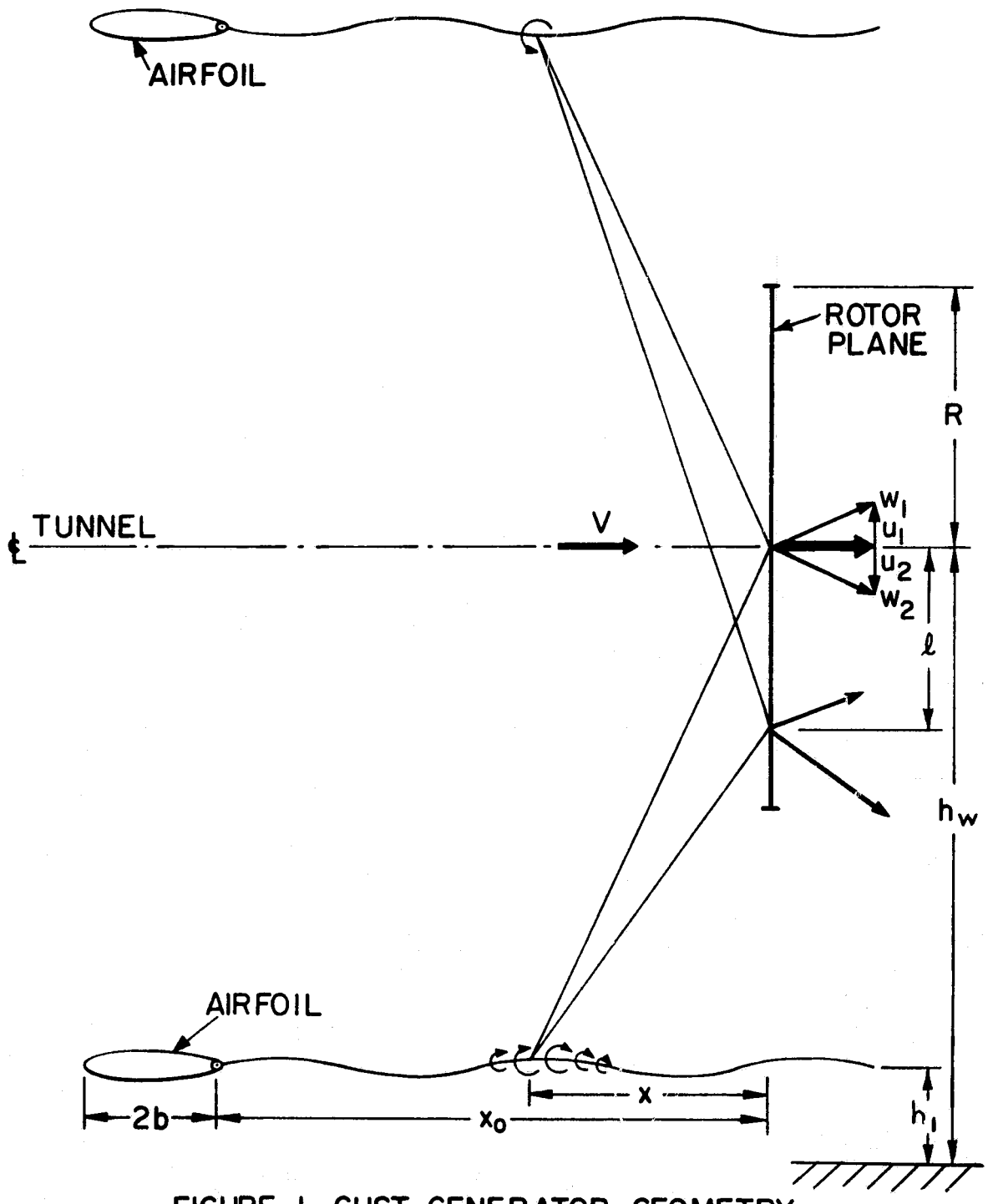

FIGURE I. GUST GENERATOR GEOMETRY

CONVENTIONAL CCA

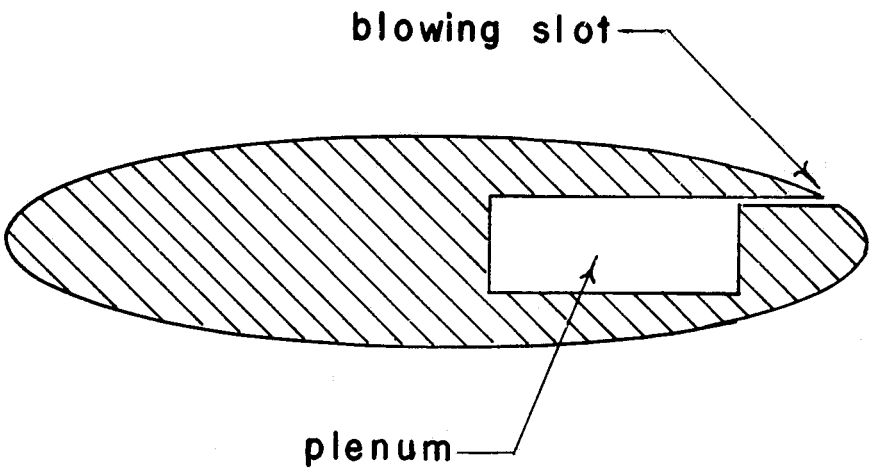

FIGURE 2a

KIND'S CCA

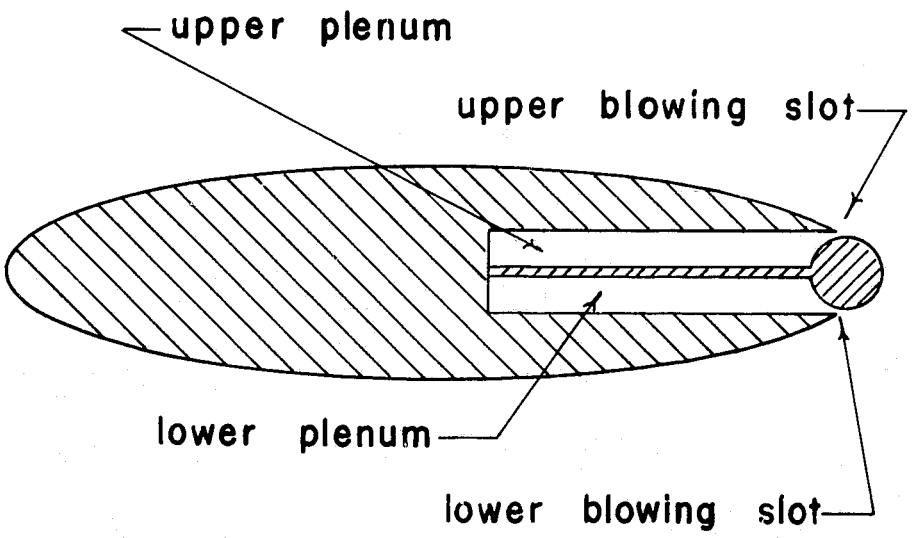

FIGURE 2b

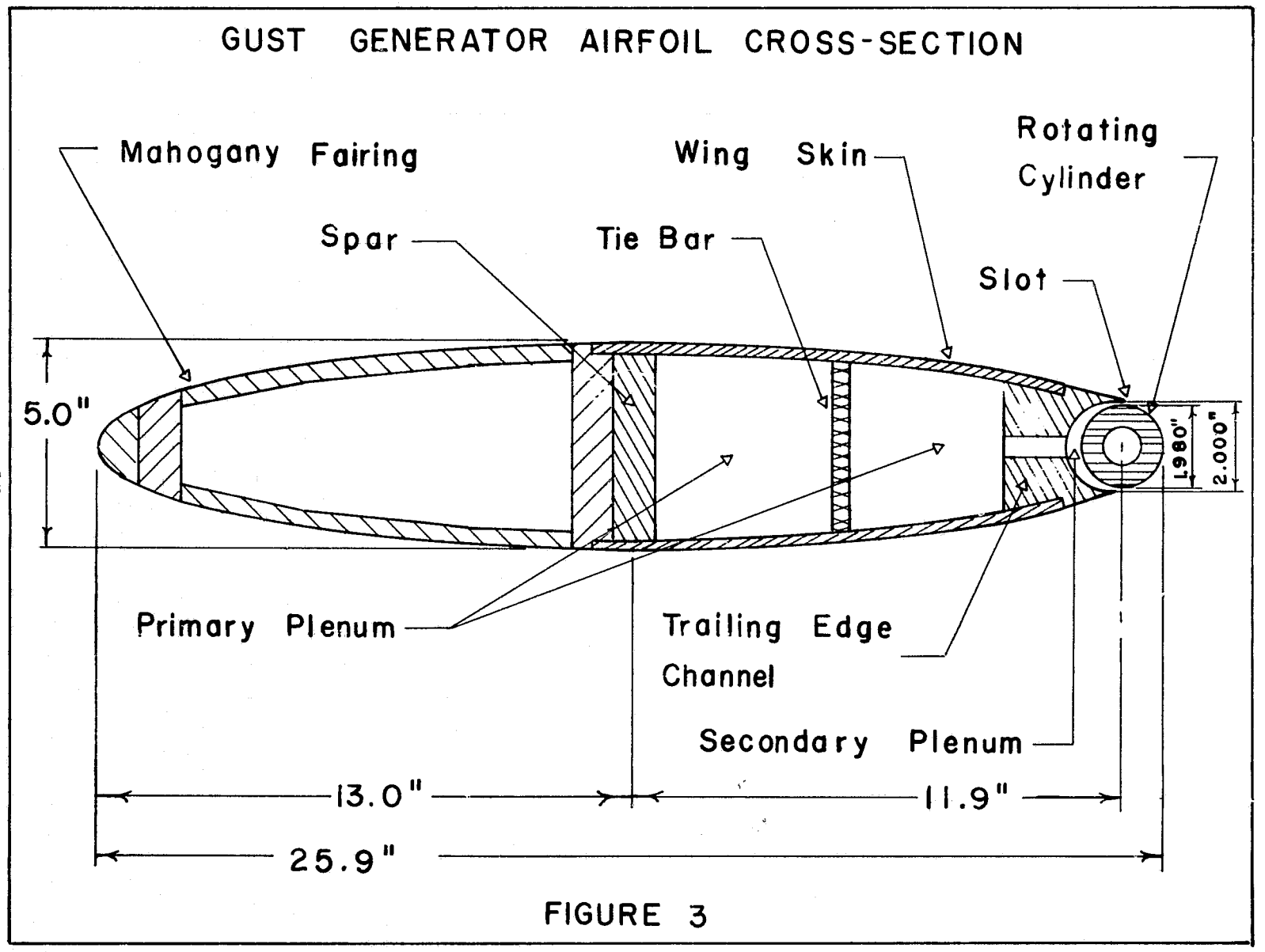
GUST GENERATOR AIRFOIL CROSS-SECTION
Mahogany Fairing
Wing Skin
Rotating Cylinder
Spar
Tie Bar
Slot
5.0"
1.980"
2.000"
Primary Plenum
Trailing Edge Channel
Secondary Plenum
13.0"
11.9"
25.9"

FIGURE 3

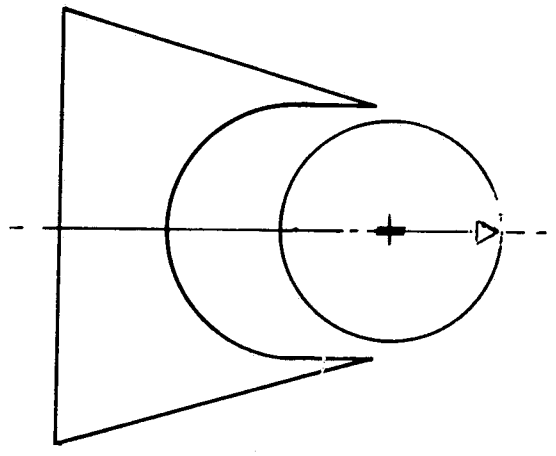

FIGURE 4a

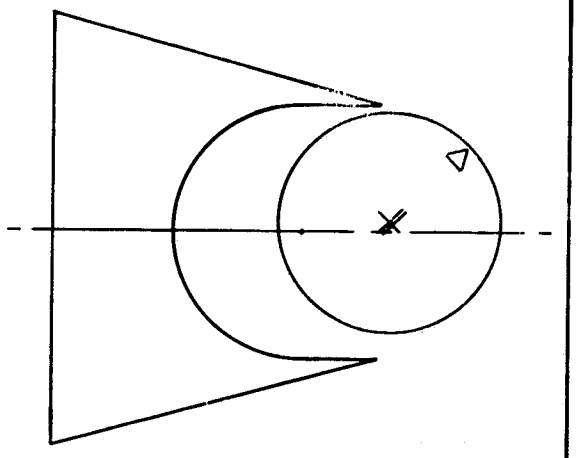

FIGURE 4b

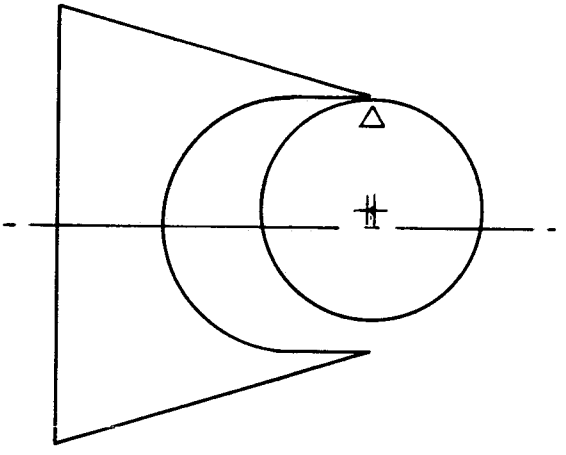

FIGURE 4c

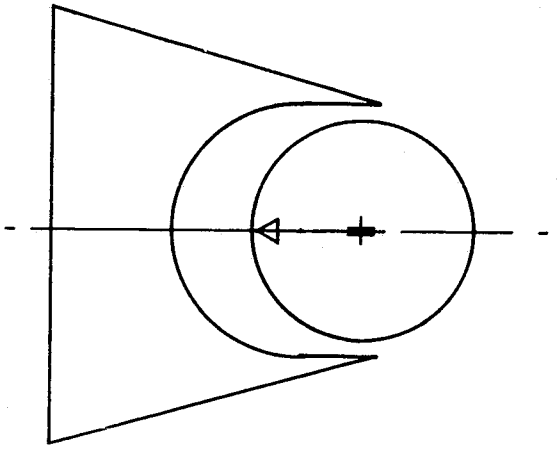

FIGURE 4d

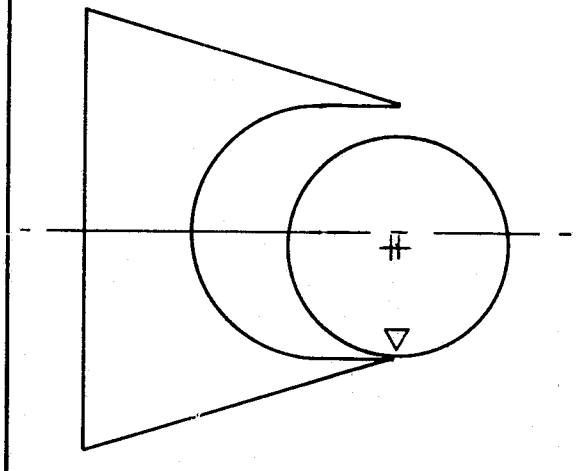

FIGURE 4e

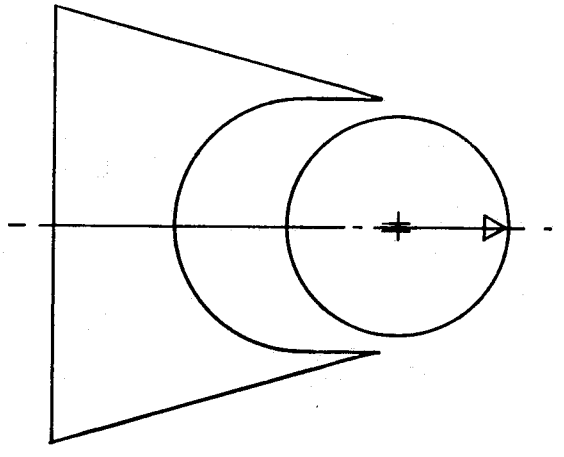

FIGURE 4f

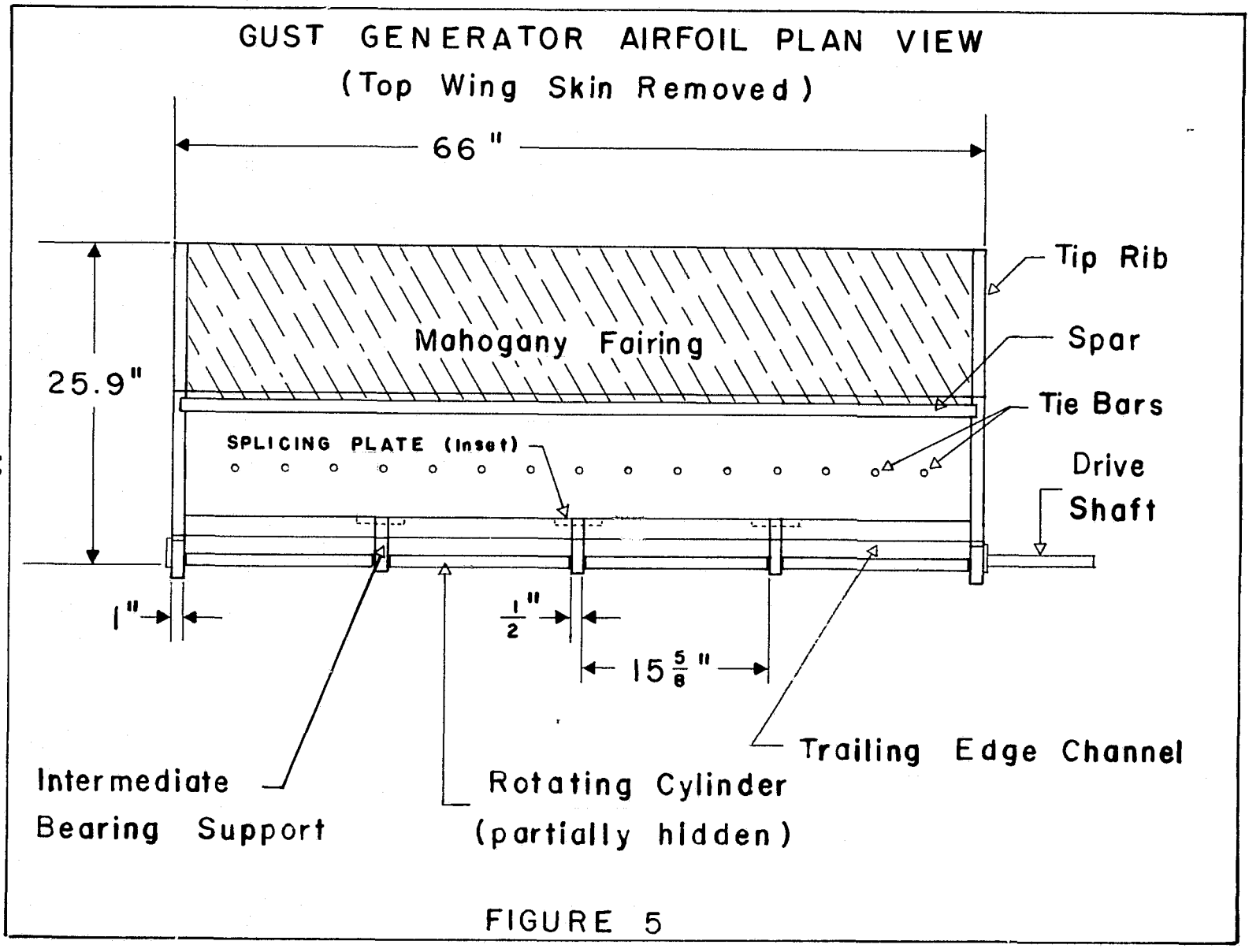
GUST GENERATOR AIRFOIL PLAN VIEW
(Top Wing Skin Removed)
66"
25.9"
Tip Rib
Mahogany Fairing
Spar
Tie Bars
SPLICING PLATE (Inset)
Drive
Shaft
1"
1/2"
15 5/8"
Trailing Edge Channel
Intermediate
Bearing Support
Rotating Cylinder
(partially hidden)

FIGURE 5

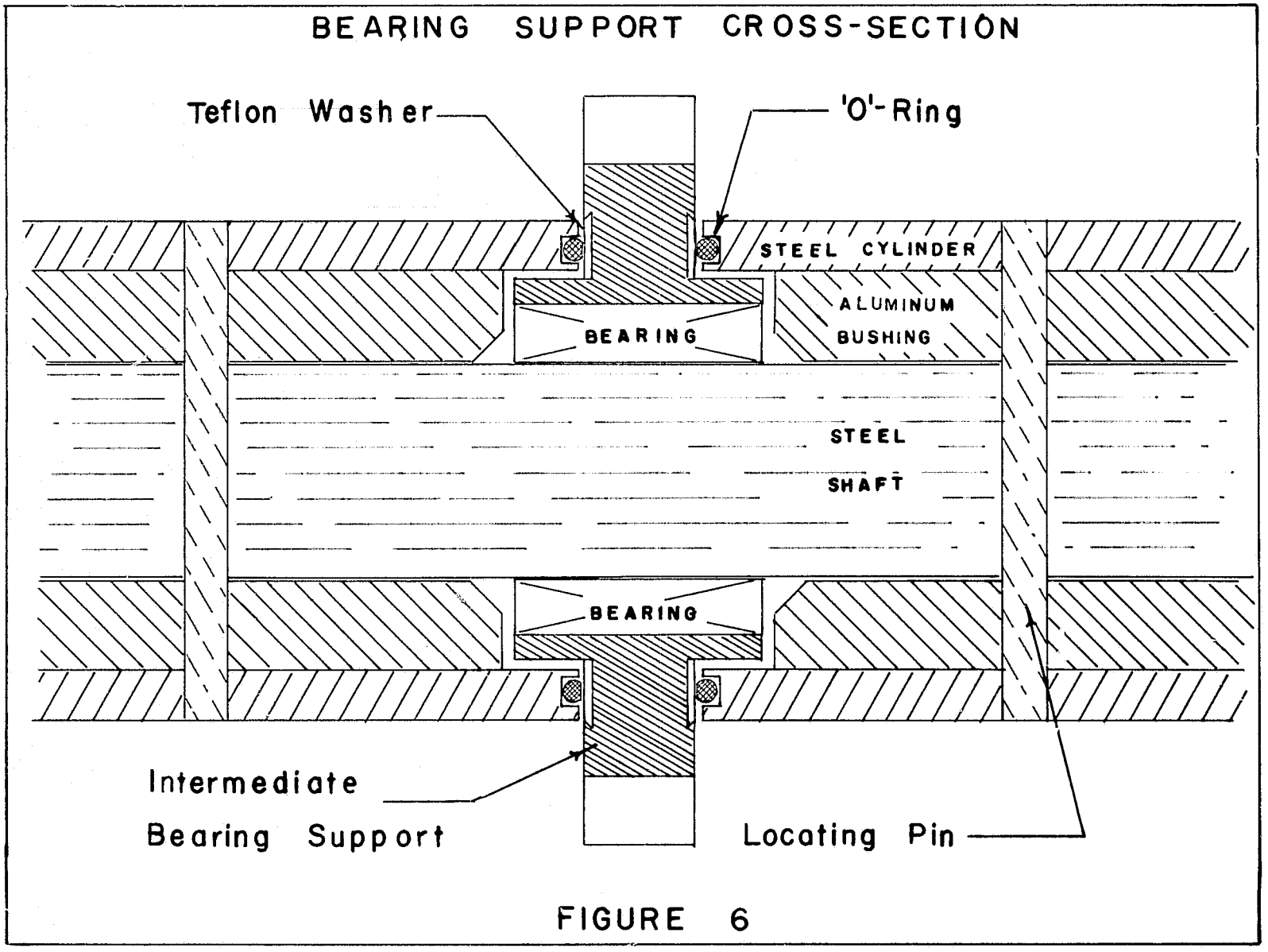
BEARING SUPPORT CROSS-SECTION
Teflon Washer
'O'-Ring
STEEL CYLINDER
ALUMINUM
BUSHING
BEARING
STEEL
SHAFT
BEARING
Intermediate
Bearing Support
Locating Pin

FIGURE 6

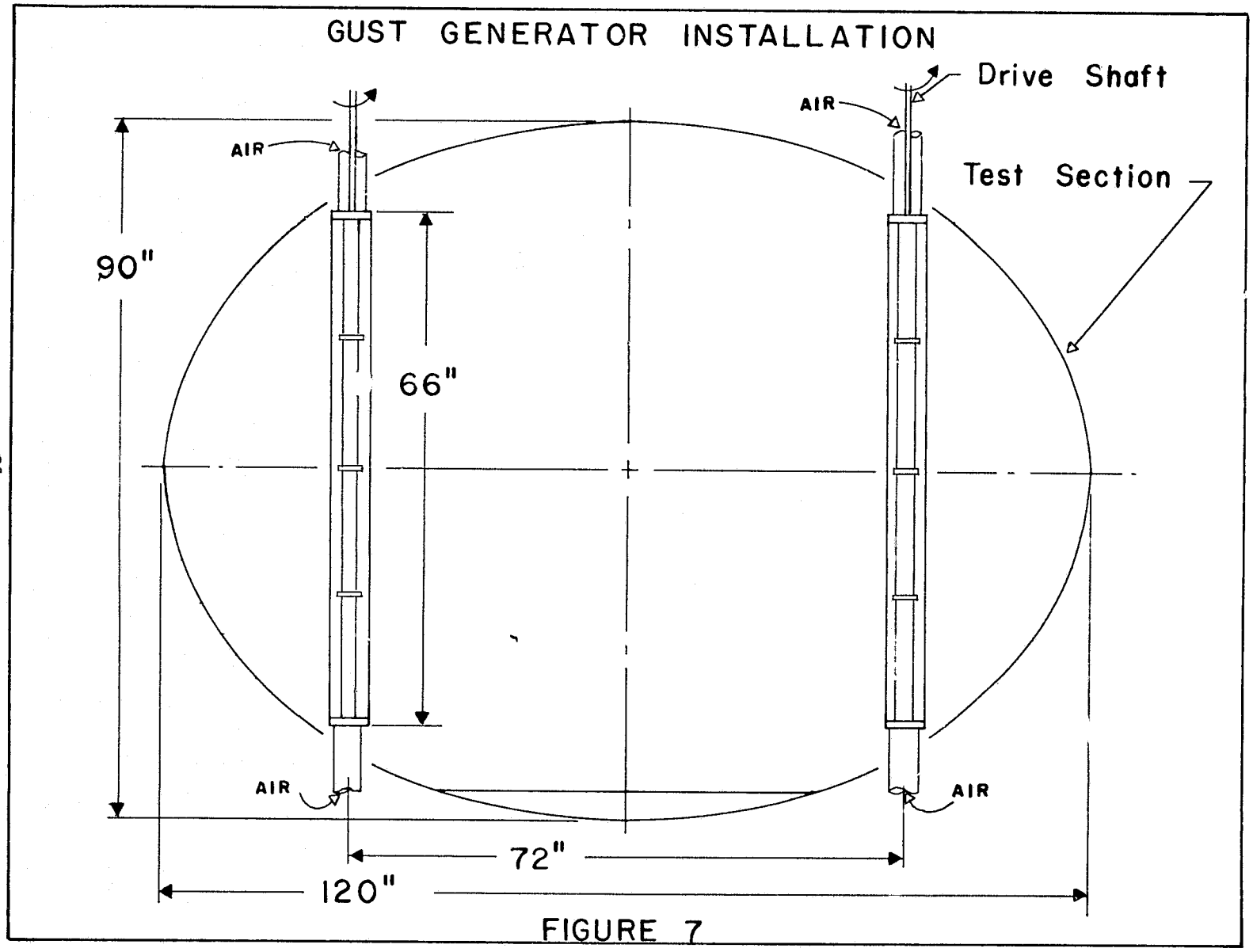
GUST GENERATOR INSTALLATION
Drive Shaft
AIR
AIR
Test Section
90"
66"
AIR
AIR
72"
120"

FIGURE 7

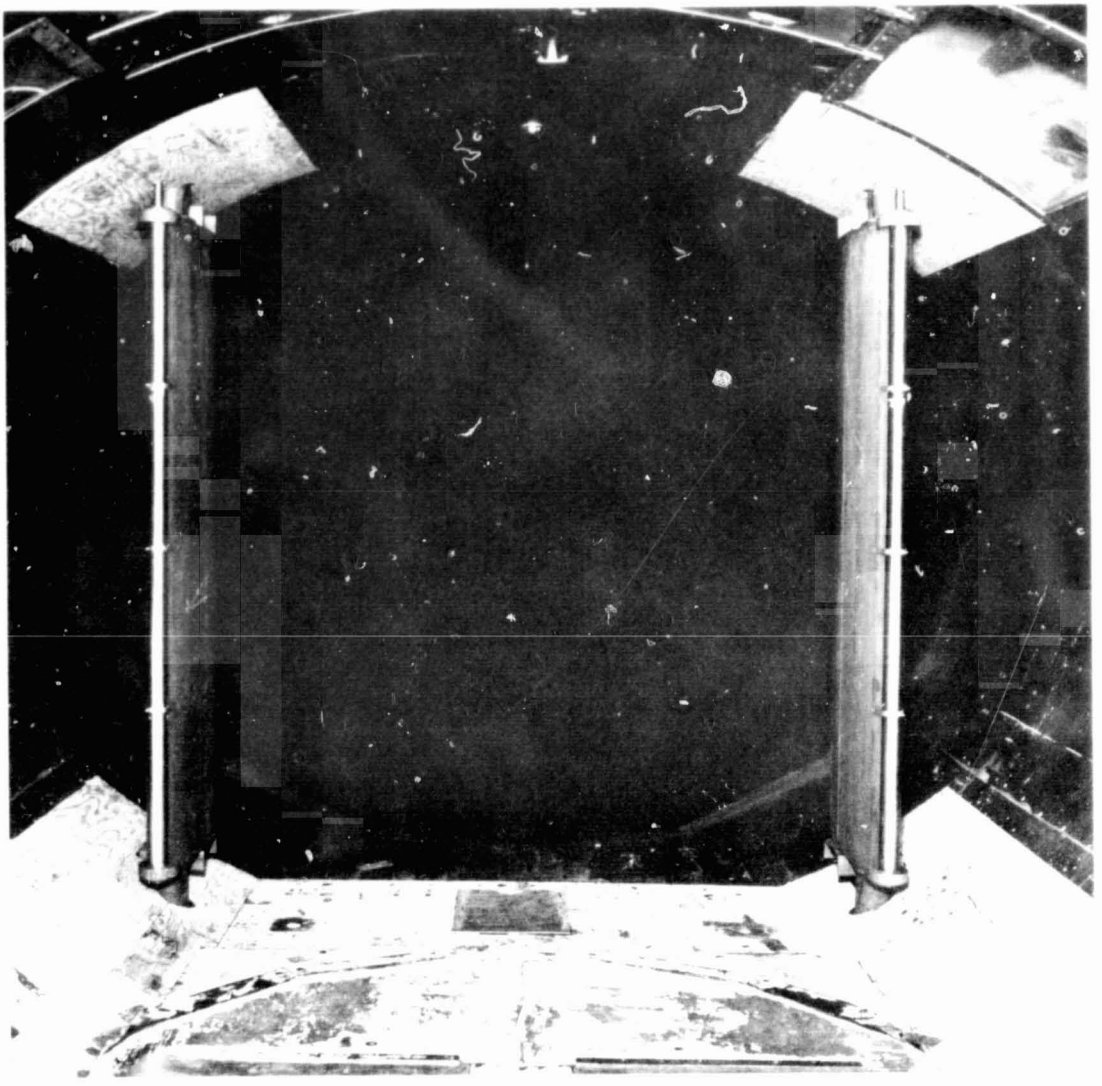

FIG. 8 GUST GENERATOR SHOWN MOUNTED IN THE WRIGHT BROTHERS WIND TUNNEL AT M.I.T.

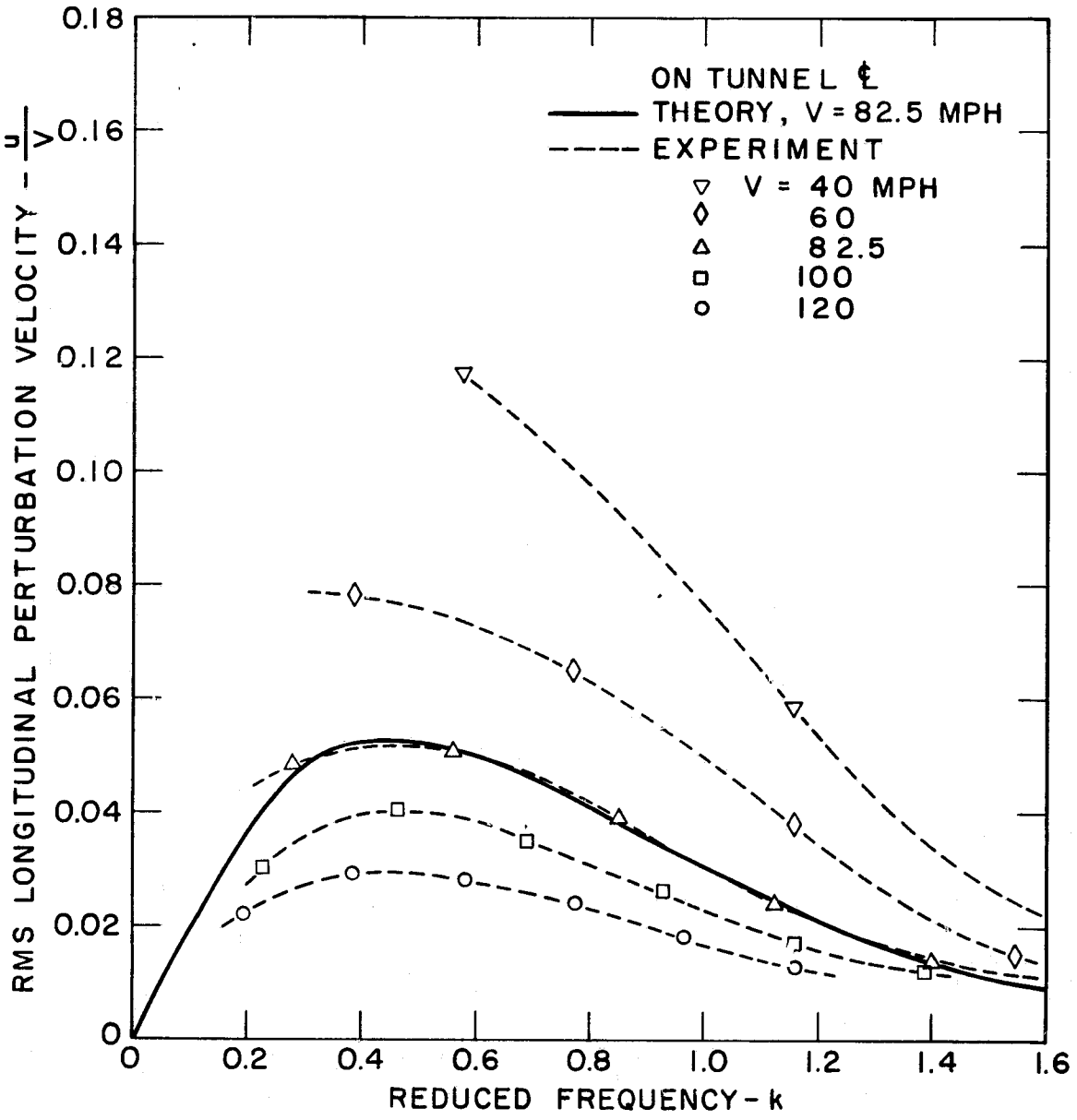

FIGURE 9 LONGITUDINAL GUST VELOCITY VERSUS REDUCED FREQUENCY

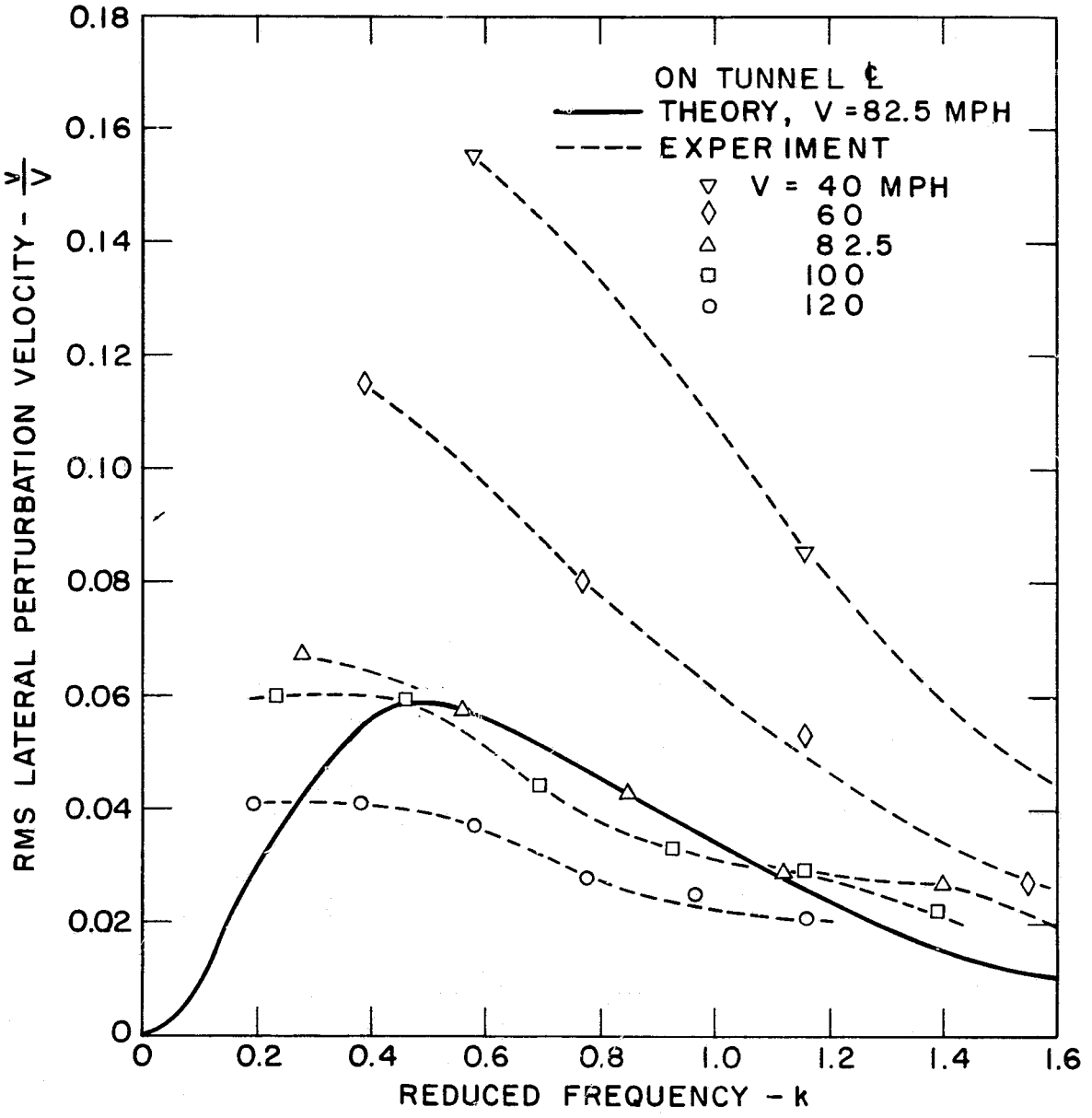

FIGURE 10 LATERAL GUST VELOCITY VERSUS REDUCED FREQUENCY

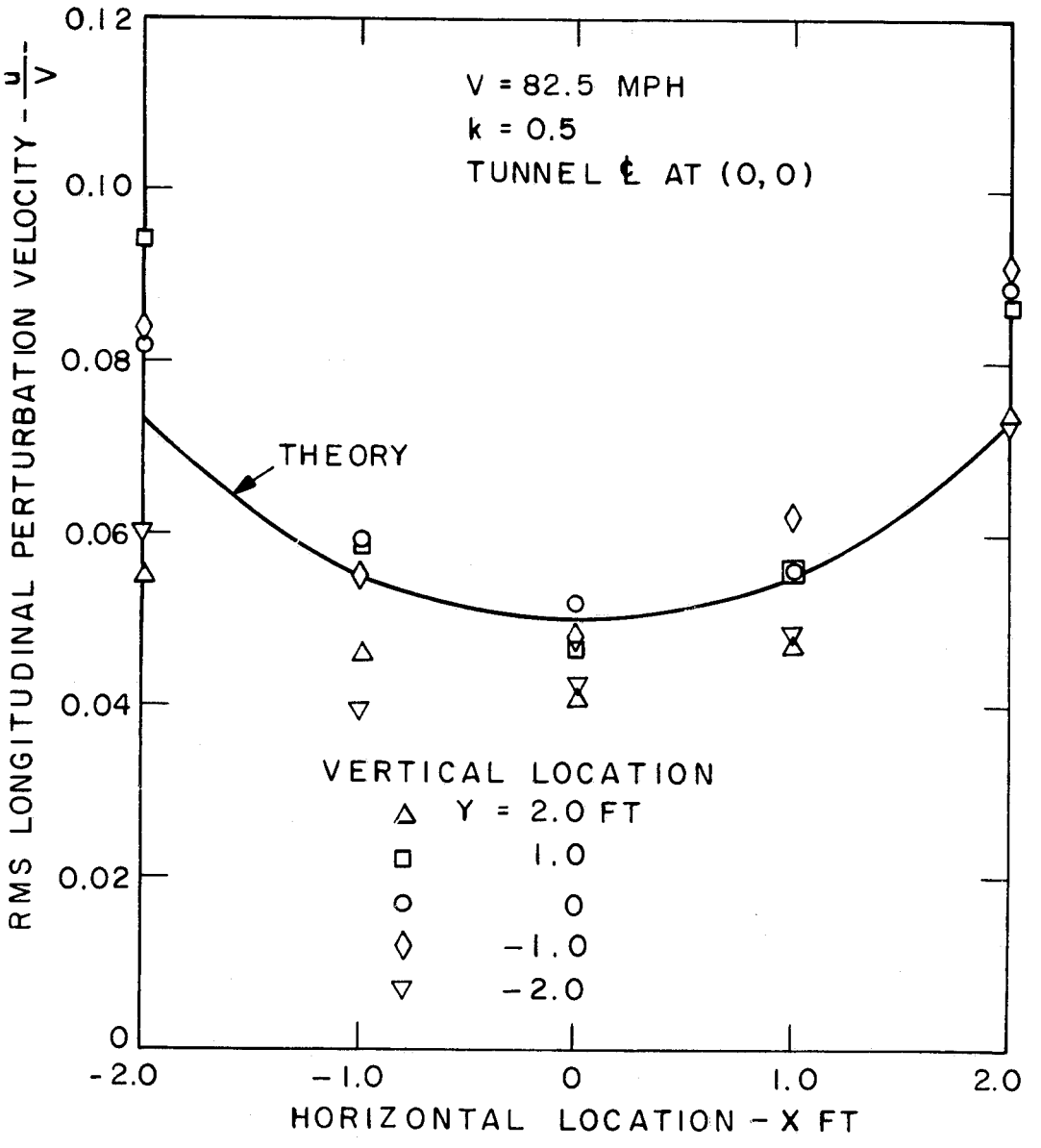

FIGURE 11 LONGITUDINAL GUST VELOCITY DISTRIBUTION, k = 0.5

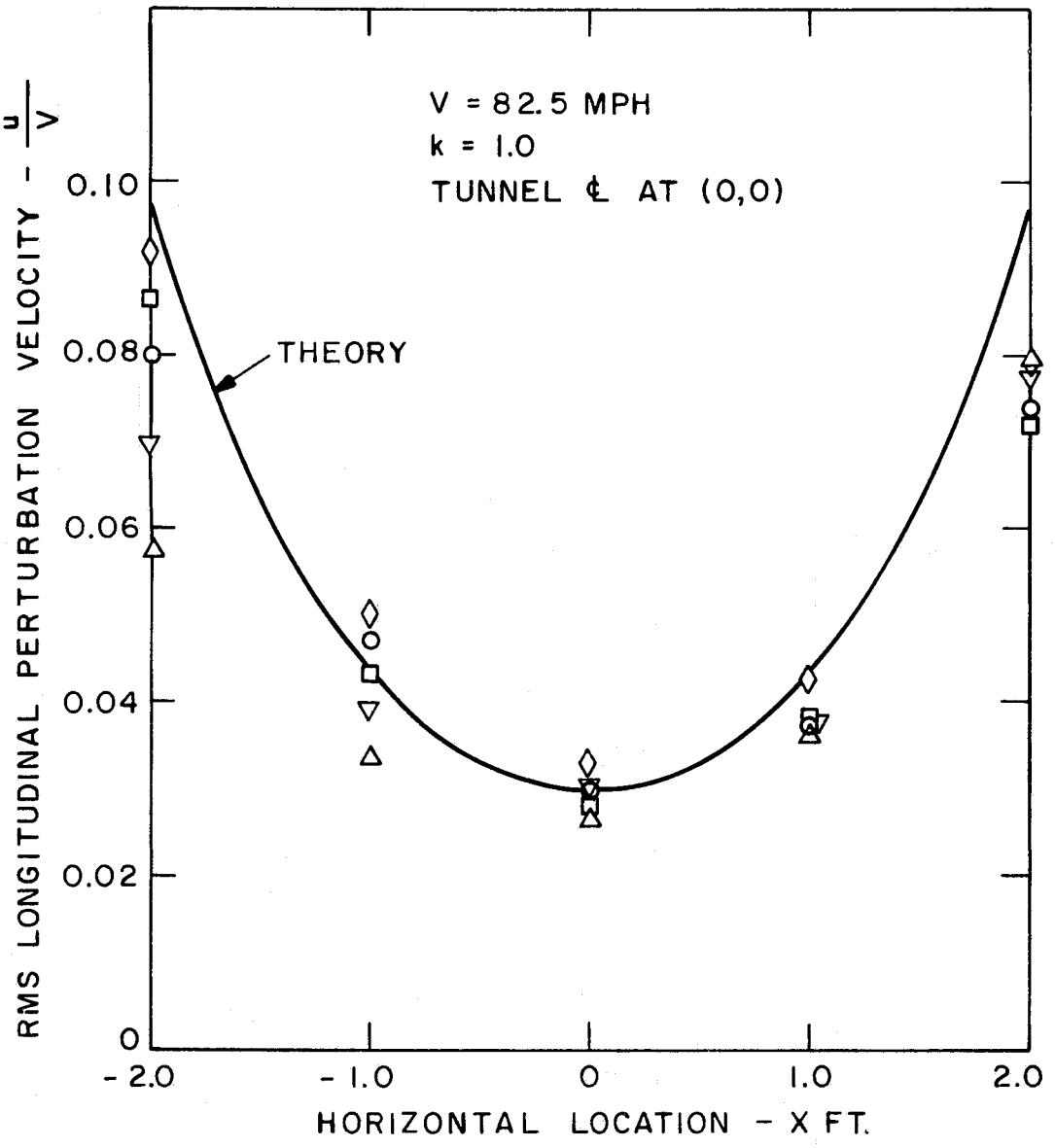

FIGURE 12 LONGITUDINAL GUST VELOCITY DISTRIBUTION, k = 1.0

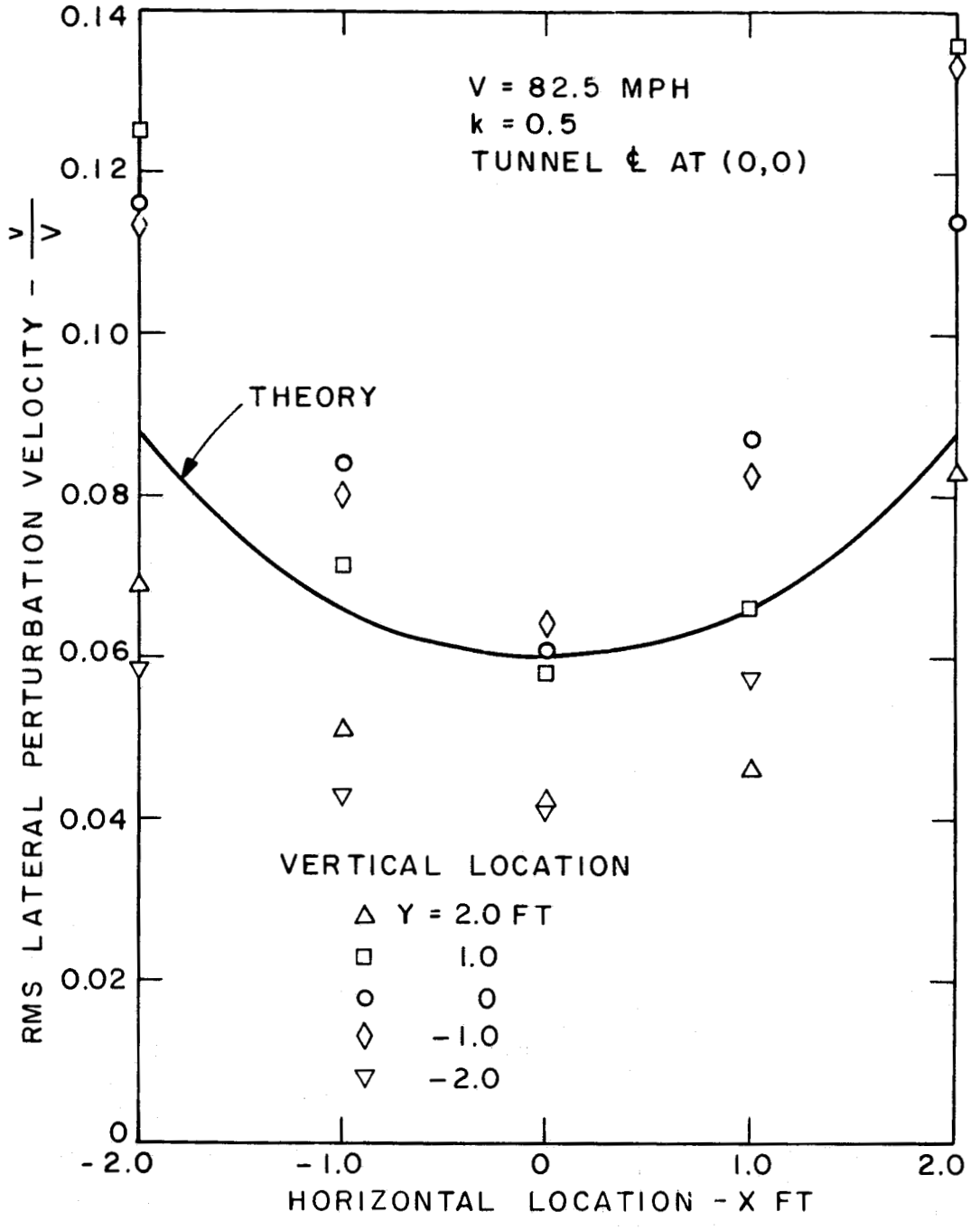

FIGURE 13 LATERAL GUST VELOCITY DISTRIBUTION, k =0.5

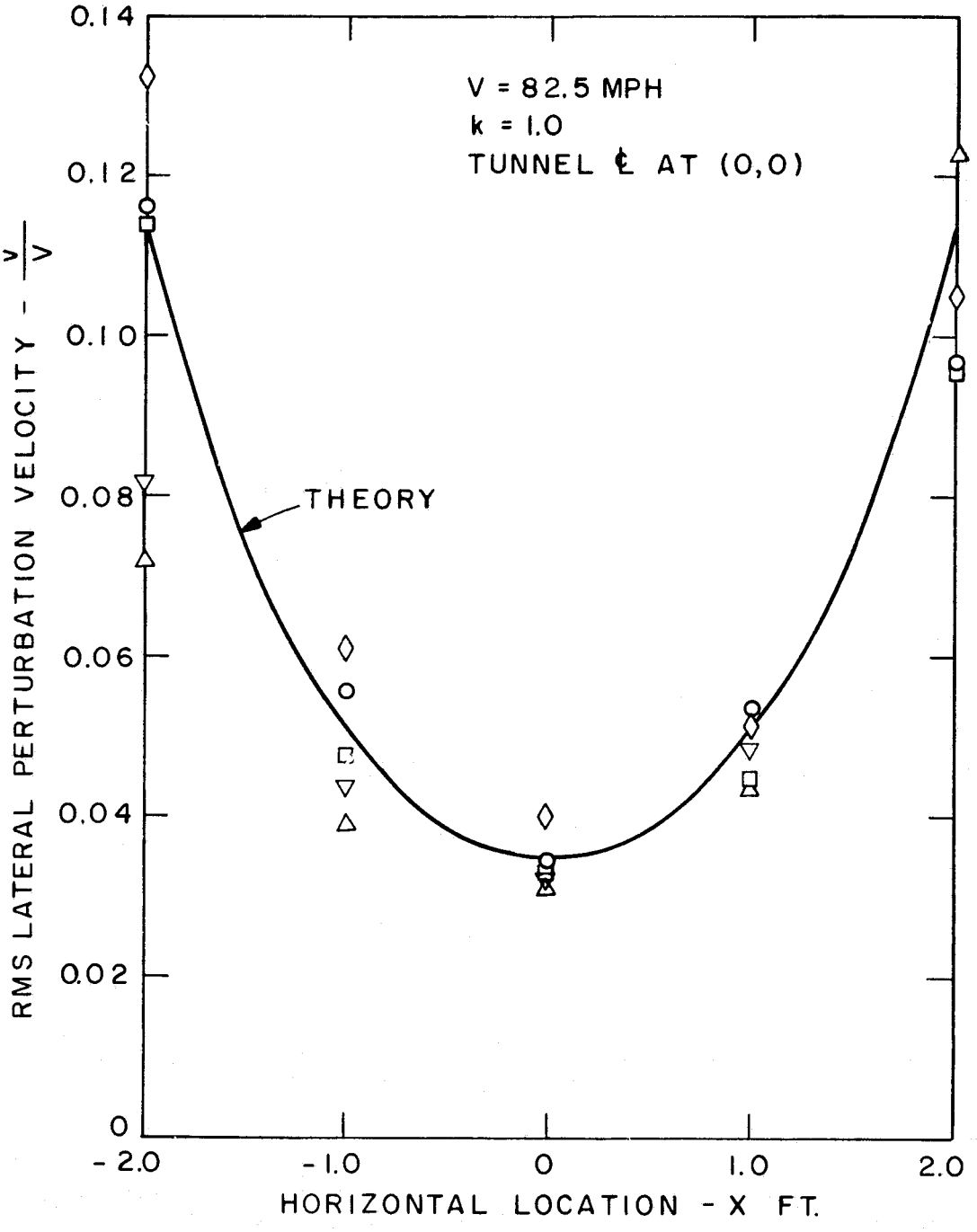

FIGURE 14 LATERAL GUST VELOCITY DISTRIBUTION, k = 1.0

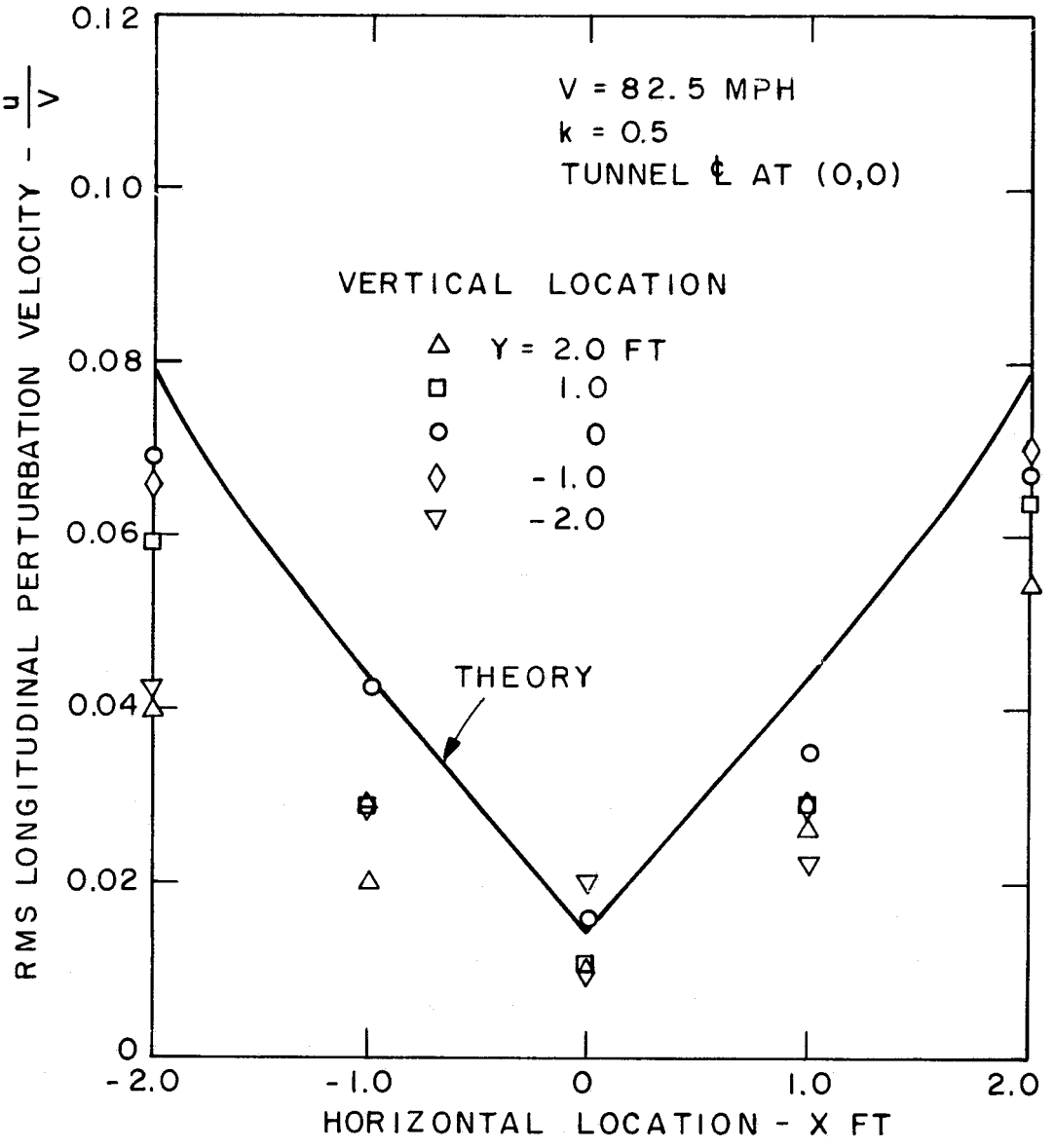

FIGURE 15 LONGITUDINAL GUST VELOCITY DURING LATERAL GENERATION, k = 0.5

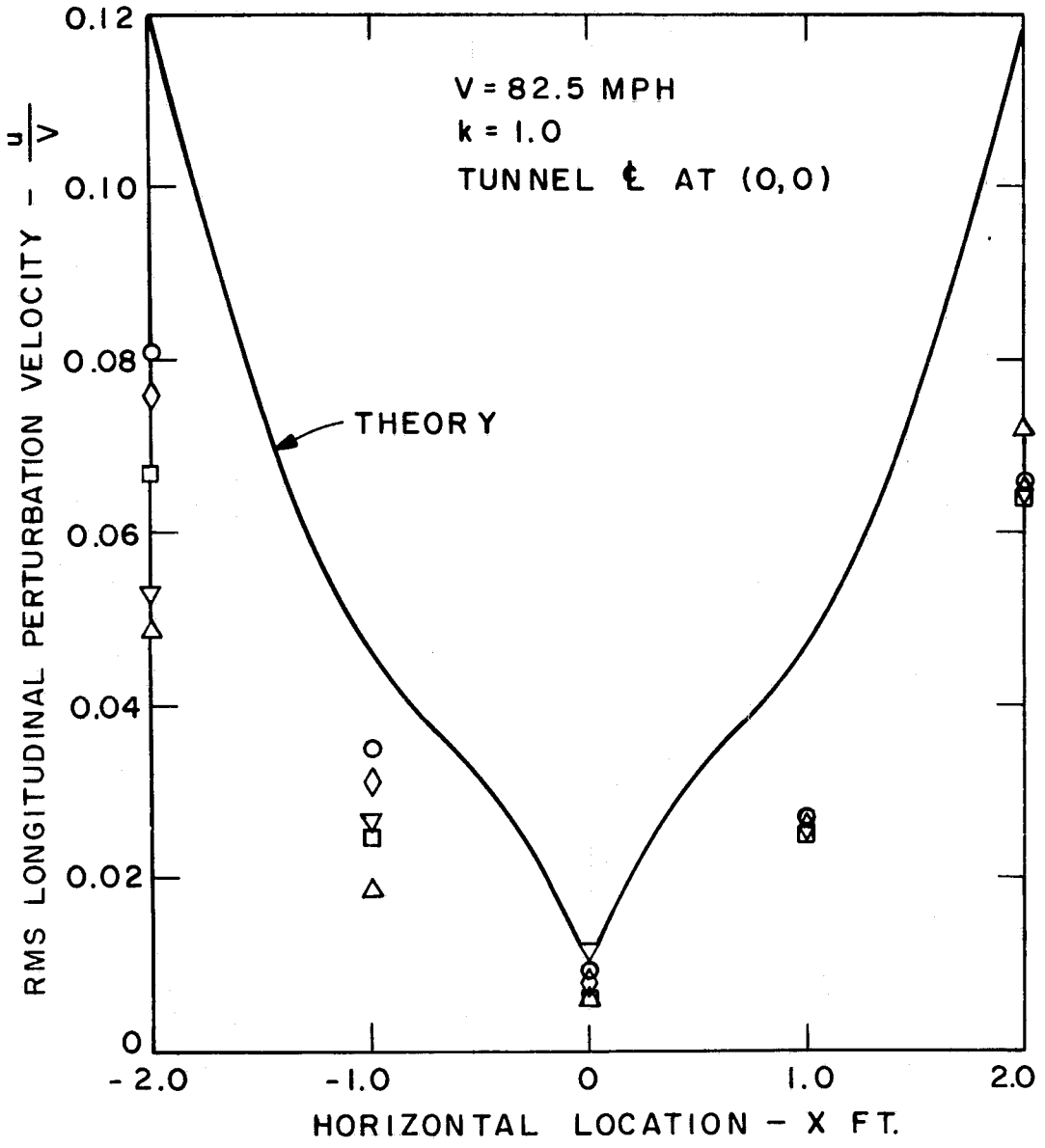

FIGURE 16 LONGITUDINAL GUST VELOCITY DURING LATERAL GENERATION, k = 1.0

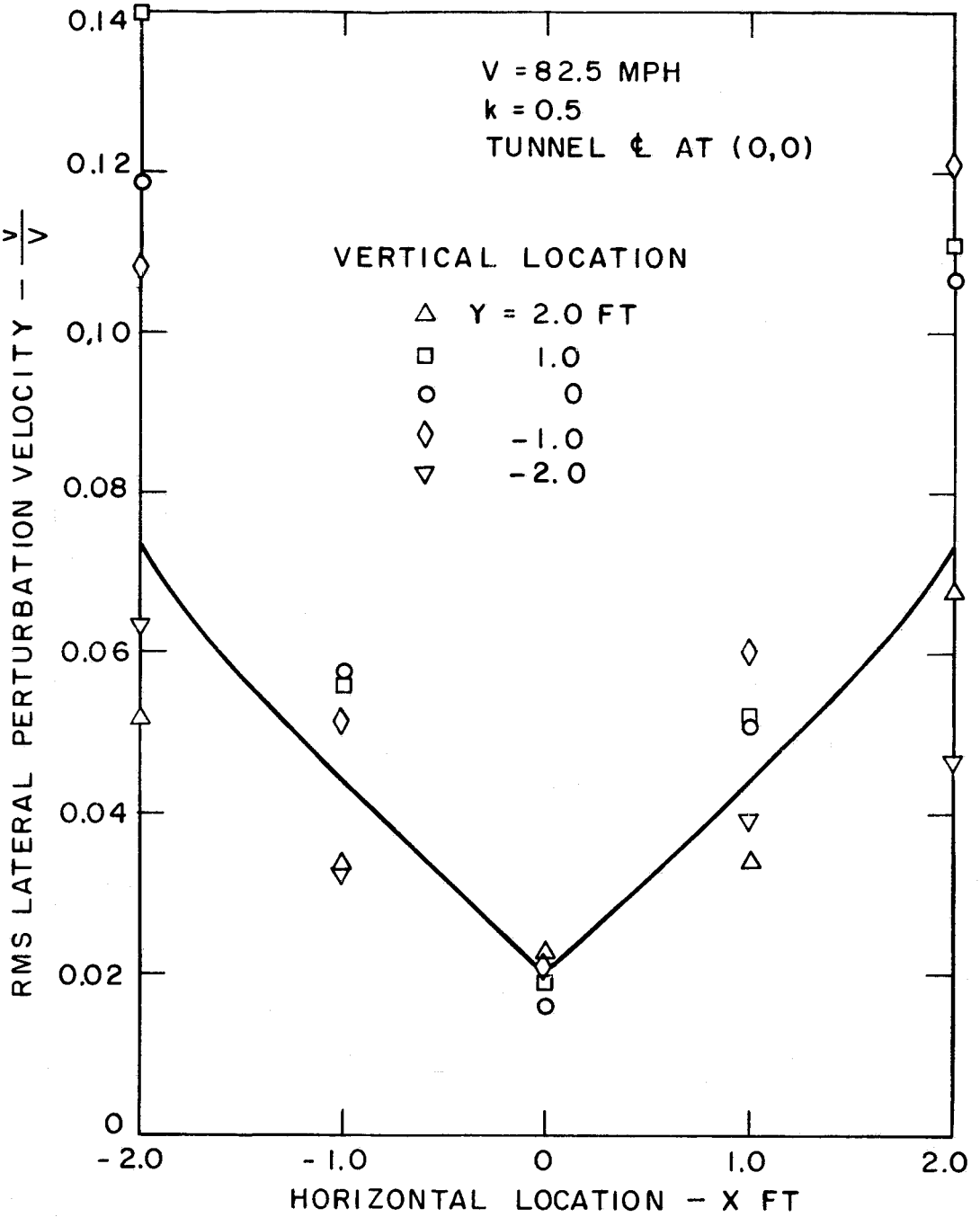

FIGURE 17 LATERAL GUST VELOCITY DURING LONGITUDINAL GENERATION, k = 0.5

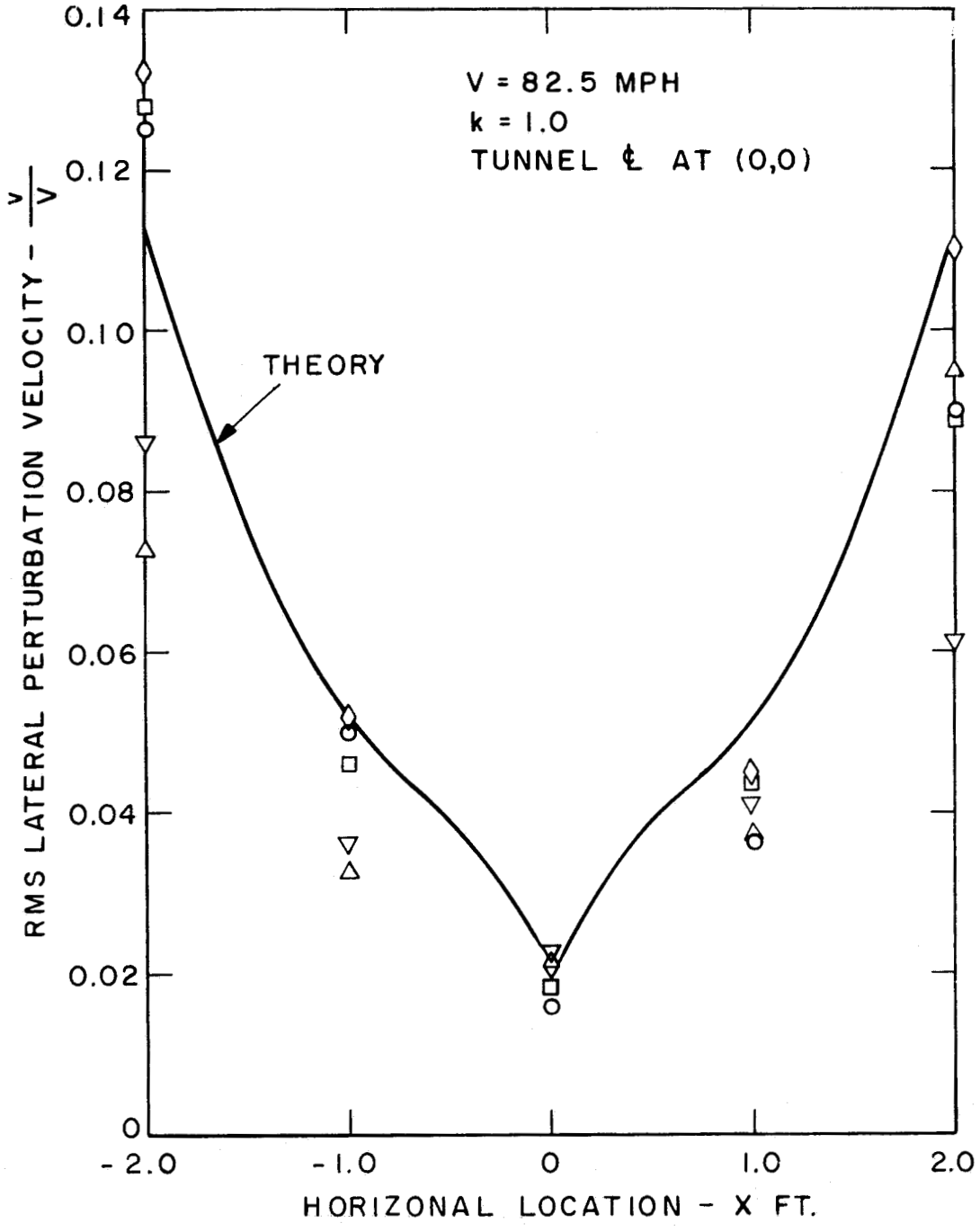

FIGURE 18 LATERAL GUST VELOCITY DURING LONGITUDINAL GENERATION k = 1.0